Table 5. Independent Risk Factors Related to the Local Control Rate: Multivariate Analysis

Factor	SE	Chi-Square Statistic	RR	95% CI	*P*
Proton therapy					
Tumor size, mm					.0030
50-100 (vs <50)	0.666	1.175	2.058	0.558-7.590	
>100 (vs <50)	0.703	10.463	9.725	2.450-38.596	
Single nodular type (vs nonsingle nodular type)	0.538	0.187	1.262	0.440-3.623	.6652
Perivascular location: Yes (vs no)	0.543	0.147	0.812	0.280-2.354	.7011
Serum PIVKAII ≥100 mAU/mL (vs <100 mAU/mL)	0.530	0.389	1.392	0.492-3.937	.5327
Carbon ion therapy					
Tumor size, mm					.4703
50-100 (vs <50)	1.569	0.069	0.662	0.031-14.322	
>100 (vs <50)	1.905	0.575	4.239	0.101-177.314	
Single nodular type (vs nonsingle nodular type)	1.231	1.110	3.658	0.328-40.853	.2921
Macroscopic vascular invasion: Yes (vs no)	1.585	0.347	2.544	0.114-56.848	.5557
All patients					
Tumor size, mm					.0002
50-100 (vs <50)	0.646	10.527	8.122	2.291-28.789	
>100 (vs <50)	0.562	2.146	0.439	0.146-1.321	
Single nodular type (vs nonsingle nodular type)	0.519	2.544	2.288	0.827-6.327	.1107
Macroscopic vascular invasion: Yes (vs no)	0.651	2.601	2.860	0.798-10.253	.1068
Perivascular location: Yes (vs no)	0.506	0.738	0.647	0.240-1.745	.3902

Abbreviations: CI, confidence interval; PIVKAII, protein induced by vitamin K absence or antagonist II; RR, relative risk; SE, standard error.

to the BED_{10} using a cutoff score of 100 (Fig. 5). The 5-year local control rates for tumors that were treated on the protocols characterized by BED_{10} values <100 and ≥ 100 were 93.3% and 87.4%, respectively, for proton therapy and 80.7% and 95.7%, respectively, for carbon ion therapy. The 5-year overall survival rates for patients who were treated on the protocols characterized by BED_{10} values <100 and ≥ 100 were 31.7% and 43.9%, respectively, for proton therapy and 32.3% and 48.4%, respectively, for carbon ion therapy. There was no significant difference in local control and overall survival rates, irrespective of the BED_{10} score, between proton therapy and carbon ion therapy.

Toxicities

All acute toxicities that occurred during treatment were transient, easily managed, and acceptable. However, grade ≥ 3 late toxicities were observed in 8 patients on proton therapy and in 4 patients on carbon ion therapy, and 4 of 12 patients were diagnosed with radiation-induced liver disease (Table 8). However, all of these patients with hematologic disorders were asymptomatic and required no further treatment. In addition, upper gastrointestinal ulcer, pneumonitis, and subcutaneous panniculitis healed with conservative management. Five patients who received proton therapy developed refractory skin ulcers, and 1 patient required skin transplantation. A salvage drainage operation also was required by 1 patient who developed infectious biloma 10 months after irradiation. No patients died of treatment-related toxicity.

DISCUSSION

We analyzed the safety and efficacy of particle therapy using proton and carbon ion beams for HCC in a single center. The key findings of this study are as follows: 1) particle therapy produced excellent local control and overall survival rates with acceptable adverse events, 2) the treatment results from carbon ion therapy appeared to be equivalent to those from proton therapy, and 3) tumor size was the only risk factor that affected the local control rate.

Local control rates for both proton therapy and carbon ion therapy exceeded 90% in the current study. These data are very similar to those related to particle therapy for HCC, whereas they are superior to data related to conformal radiotherapy.[16,18,29,30] Recent improvements in dose localization techniques, such as intensity-modulated radiotherapy, conformal 3-dimensional planning, and breathing motion management strategies, thus, have made it possible to irradiate smaller, well defined targets in the liver. However, these highly computer-assisted

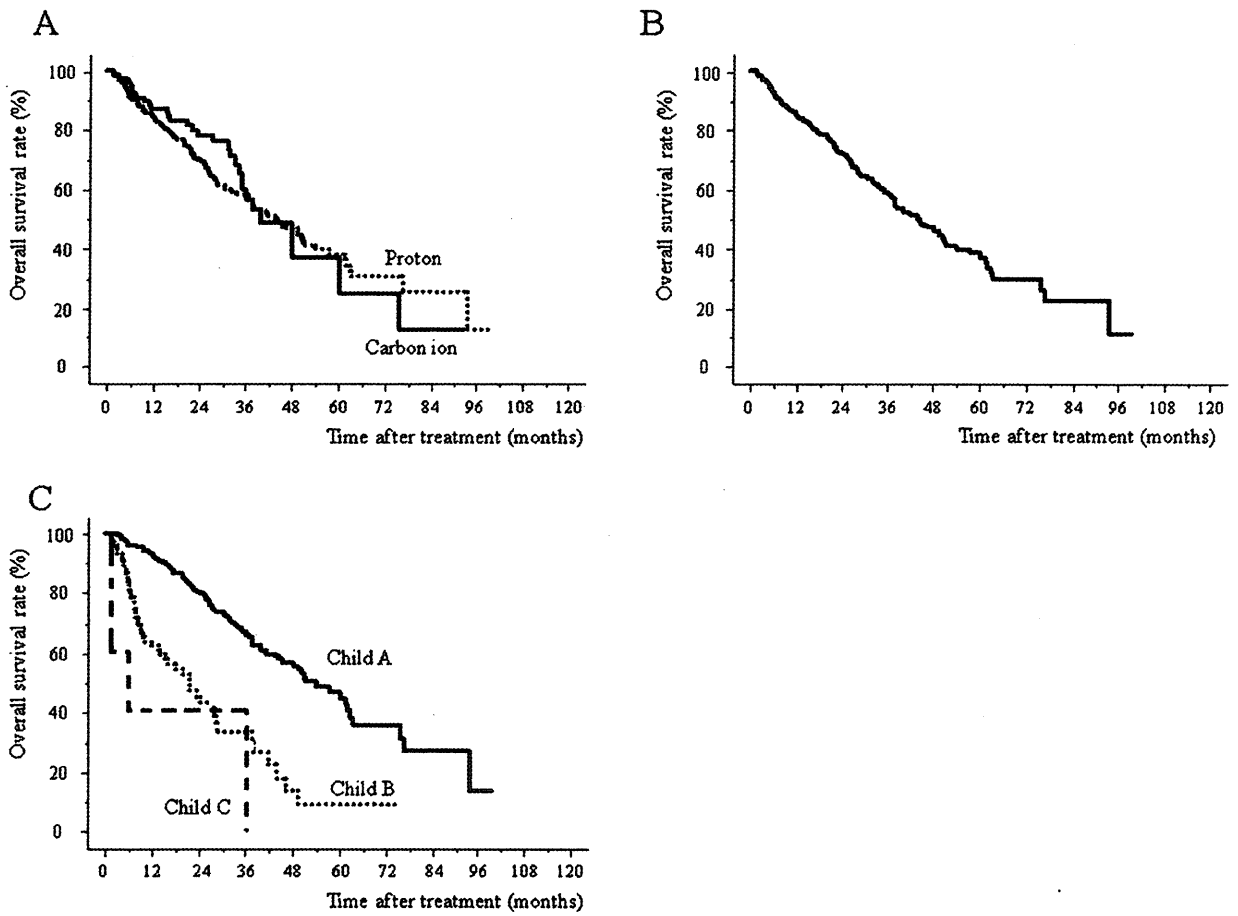

Figure 3. Overall survival rates after treatment are illustrated for (A) patients who received with proton and carbon ion therapy, (B) all 343 patients, and (C) all 343 patients according to Child-Pugh classification.

irradiation techniques using photon beams have achieved limited efficacy in treating patients with HCC. The local control rates produced by these conformal approaches remain in the 40% to 66% range for several reasons.[29,30] Radiation-induced liver disease still is observed frequently with conformal approaches when a sufficient dose is delivered to completely kill the cells of the entire tumor nodule. This is especially the true for large and centrally situated liver tumors.[31] In this regard, particle beams can achieve an excellent dose distribution to these targets. The area of radiation dose deposition can be controlled well by the beam energy, because there is a rapid drop-off in energy deposition beyond the target area. Indeed, such theoretical advantages of particle therapy were proven in part by the impressively high local control rate of approximately 90% in the current study. Therefore, we believe that it is reasonable to say that the tumor-eliminating capability of particle therapy is closely equivalent to that of hepatectomy, an outcome that has not been achieved with other radiation therapies.

Experience in the treatment of HCC by particle therapy has been accumulated mainly in Japanese centers, but there is increasing interest in other countries as well. There were 26 active proton therapy facilities as of February 2009, whereas there were only 3 carbon ion therapy facilities.[32] Until now, several proton treatment centers and 1 carbon ion treatment center have reported HCC treatments results.[16-19] However, except for the HIBMC, no single facility can deliver both proton and carbon ion beams. Therefore, our facility has a distinct advantage over other institutes with regard to comparing the efficacy of the 2 beams. To select proton therapy or carbon ion therapy, we made treatment plans for both proton and carbon ion therapy. When dose distributions were

Table 6. Univariate Analysis of Prognostic Factors for Overall Survival Rate

Factor	Proton Therapy, n=242		Carbon Ion Therapy, n=101		All Patients, n=343	
	OS Rate at 5 Years, %	*P*	OS Rate at 5 Years, %	*P*	OS Rate at 5 Years, %	*P*
Age, y		.7986		.6769		.6448
<70	37.3		43.9		39.4	
≥70	38.2		26.9		36.2	
Positive viral marker		.9754		.1805		.8586
Hepatitis B virus	34.9		44.6		32.4	
Hepatitis C virus	35.8		40.8		36.3	
None	46.7		33.9		46.6	
Performance status		<.0001		.2295		<.0001
0	43.5		43.7		43.6	
1 or 2 or 3	24.8		26.8		24.1	
Child-Pugh classification		<.0001		<.0001		<.0001
A	46.8		41.2		46.6	
B or C	8.2		33.3		8	
Tumor size, mm		.1438		.0003		.0038
<50	37.8		53.5		39.2	
50-100	37.4		17.9		33.8	
>100	41.1		0		39.8	
Macroscopic vascular invasion		.0003		.0055		<.0001
Yes	33.2		22		31.5	
No	40.3		47.8		40.2	
Serum AFP, ng/mL		.0026		.0024		<.0001
<100	42		30.9		42.6	
≥100	29.5		23.1		28.9	
Serum PIVKAII, mAU/mL		.0109		.4041		.0082
<100	40.4		58.4		41.8	
≥100	35.5		16.5		33.8	

Abbreviations: AFP, α-fetoprotein; OS, overall survival; PIVKAII, protein induced by vitamin K absence or antagonist II.

compared, there were many instances in which low-dose areas had spread into the surrounding normal liver during proton therapy planning. This was apparently because of the relatively large penumbra of proton beams. Consequently, dose distribution in a single beam appears to be better in carbon ion therapy than in proton therapy. However, in terms of beam arrangement, carbon ions are emitted from 3 fixed ports, such as vertical, horizontal, or 45-degree oblique; whereas a 360-degree rotating gantry can be used for protons. The high positioning accuracy achieved by irradiating patients in a supine position also was an advantage of proton therapy. Currently, 360-degree rotating gantries for carbon ion beams are under construction in Japan and Germany, and it is expected that these will enable the delivery of highly precise carbon ion beam arrangements and, thus, will improve the effectiveness of carbon ion therapy for HCC.

In addition to dose distribution, there are evident differences in biologic properties between the 2 beams, ie, the RBE. The RBE for proton therapy is comparatively simple. The International Commission on Radiation Units and Measurements has recommended 1.1 as a generic RBE for proton therapy based on an analysis of the published RBE values determined from in vivo systems.[33,34] All proton therapy centers, including the HIBMC, have accepted this recommendation. Conversely, the RBE for carbon ion therapy is complex, because there is no common model for selecting the RBE of carbon ion beams. In addition, it may vary depending on tissue type and the depth of the spread-out Bragg peaks.[32] Because of these differences, planning the physical dose distribution is substantially more complex for carbon ion beams than for proton beams; therefore, a direct comparison of proton therapy and carbon ion therapy is

Table 7. Independent Risk Factors Related to the Overall Survival Rate: Multivariate Analysis

Factor	SE	Chi-Square Statistic	RR	95% CI	*P*
Proton therapy					
Performance status 1-3 (vs 0)	0.200	9.283	0.544	0.368-0.805	.0023
Child-Pugh classification B or C (vs A)	0.204	29.731	0.329	0.220-0.490	<.0001
Macroscopic vascular invasion: Yes (vs no)	0.203	9.410	0.536	0.360-0.799	.0022
Serum AFP ≥100 ng/mL (vs <100 ng/mL)	0.198	2.281	1.349	0.915-1.990	.1310
Serum PIVKAII ≥100 mAU/mL (vs <100 mAU/mL)	0.199	1.231	1.248	0.844-1.844	.2672
Carbon ion therapy					
Child-Pugh classification B or C (vs A)	0.519	17.642	0.113	0.041-0.313	<.0001
Tumor size, mm					.0297
50-100 (vs <50)	0.569	6.795	4.412	1.445-13.468	
>100 (vs <50)	1.040	3.217	6.454	0.841-49.524	
Macroscopic vascular invasion: Yes (vs no)	0.625	0.647	1.654	0.486-5.631	.4211
Serum AFP ≥100 ng/mL (vs <100 ng/mL)	0.396	5.406	2.513	1.156-5.465	.0201
All patients					
Performance status 1-3 (vs 0)	0.180	10.852	0.554	0.389-0.787	.0010
Child-Pugh classification B or C (vs A)	0.182	45.663	0.292	0.204-0.417	<.0001
Tumor size, mm					.5976
50-100 (vs <50)	0.220	0.044	1.047	0.680-1.613	
>100 (vs <50)	0.375	0.656	0.738	0.354-1.539	
Macroscopic vascular invasion: Yes (vs no)	0.216	10.960	0.489	0.320-0.747	.0009
Serum AFP ≥100 ng/mL (vs <100 ng/mL)	0.176	4.848	1.474	1.044-2.083	.0277
Serum PIVKAII ≥100 mAU/mL (vs <100 mAU/mL)	0.186	0.922	1.196	0.830-1.724	.3371

Abbreviations: AFP, α-fetoprotein; CI, confidence interval; PIVKAII, protein induced by vitamin K absence or antagonist II; RR, relative risk; SE, standard error.

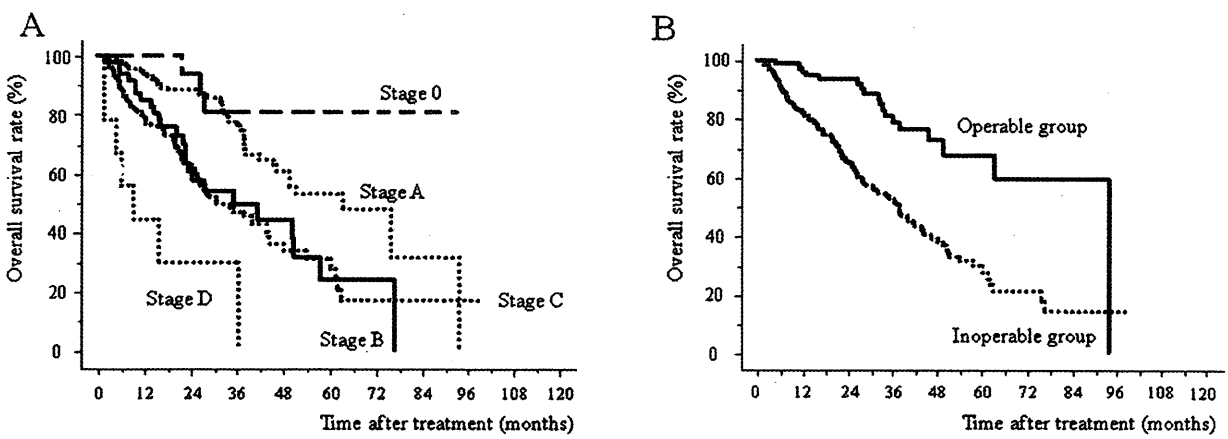

Figure 4. (A) Overall survival rates are illustrated for all 343 patients according to disease stage classified by the Barcelona Clinic Liver Cancer classification. (B) Overall survival rates are illustrated for all 343 patients according to the operative indication based on the Barcelona Clinic Liver Cancer classification.

not feasible. Under these circumstances, we established that the treatment results of carbon ion therapy were equivalent to those of proton therapy at our institute. These results may prove the validity of our treatment planning system for carbon ion therapy by using a variable RBE.

The current study has established the equal effectiveness of proton and carbon ion therapies for HCC. With regard to this result, we speculate that the superior dose distribution compensates for the limitation of carbon ion beam arrangements at HIBMC. With the development of irradiation equipment, compared with proton therapy, carbon ion therapy will play a major role in the treatment of patients with HCC who have tumors adjacent to the gut and/or those whose liver function has deteriorated. However, carbon ion therapy requires huge economic resources, and this issue should be resolved in the future.

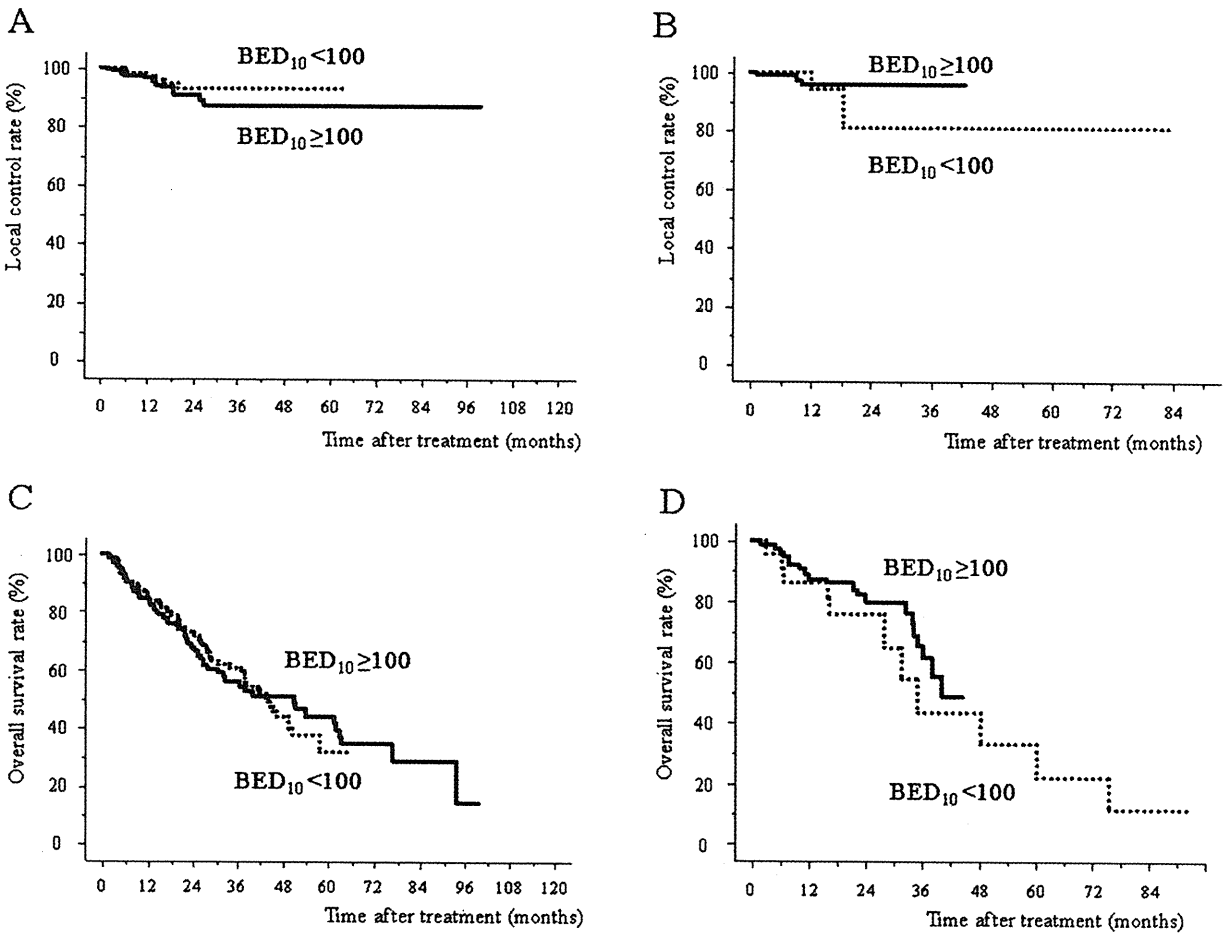

Figure 5. Local control rates are illustrated according to the radiobiologic equivalent dose for acute-reacting tissues (BED_{10}) for (A) proton therapy and (B) carbon ion therapy. Overall survival rates are illustrated according to the BED_{10} for (C) proton therapy and (D) carbon ion therapy.

Tumor size was the only significant risk factor for local recurrence after particle therapy (for proton therapy, carbon ion therapy, and all patients). Conversely, it is noteworthy that the 6 other tumor factors, including gross classification, macroscopic vascular invasion, perivascular location, prior treatment history, serum AFP levels, and serum PIVKAII levels, had no significant influence on the local control rate after either therapy. The application of local ablative therapies is contraindicated in tumors with vascular invasion,[9,35] and it has been reported by several studies that perivascular location significantly increased the local recurrence rate after RFA mainly because of the heat-sink effect.[8,9] In addition, hepatectomy frequently is abandoned to as a treatment for centrally situated tumors adjacent to the inferior vena cava and/or the main portal trunk in patients with cirrhosis, because these tumor locations tend to require major hepatectomy. In the current study, however, neither factor reduced the efficacy of proton therapy or carbon ion therapy in terms of the local control rate.

The local control rates achieved with proton therapy and carbon ion therapy for tumors <50 mm were 95.5%, and 94.5%, respectively. These data are similar or superior to those reported with local ablative therapies.[36] At the same time, the local control rates achieved with proton therapy and carbon ion therapy for tumors that measured from 50 mm to 100 mm in greatest dimension were 84.1% and 90.9%, respectively (Table 4). Because the upper limit of tumor size is 50 mm for local ablative therapies, these results clearly demonstrate the distinct advantage of particle therapy over other local therapies for tumors ≥50 mm. Taken together, in our opinion, particle

Table 8. Late Toxicities After Proton and Carbon Ion Therapy

	No. of Patients (%)								
	Grade 2			Grade 3			Grade 4		
Toxicity	Proton Therapy	Carbon Ion Therapy	All Patients	Proton Therapy	Carbon Ion Therapy	All Patients	Proton Therapy	Carbon Ion Therapy	All Patients
Dermatitis	12 (5)	5 (5)	17 (5)	4 (2)	0	4 (1)	1 (1)	0 (0)	1 (1)
Elevation of transaminase level	5 (2)	3 (3)	8 (2)	1 (1)	3 (3)	4 (1)	0 (0)	0 (0)	0 (0)
Upper gastrointestinal ulcer	3 (1)	1 (1)	4 (1)	1 (1)	0 (0)	1 (1)	0 (0)	0 (0)	0 (0)
Rib fracture	8 (3)	3 (3)	11 (3)	0 (0)	0 (0)	0 (0)	0 (0)	0 (0)	0 (0)
Pneumonitis	4 (2)	2 (2)	6 (2)	0 (0)	0 (0)	0 (0)	0 (0)	0 (0)	0 (0)
Subcutaneous panniculitis	6 (2)	2 (2)	8 (2)	0 (0)	1 (1)	1 (1)	0 (0)	0 (0)	0 (0)
Biloma	0 (0)	0 (0)	0 (0)	1 (1)	0 (0)	1 (1)	0 (0)	0 (0)	0 (0)
Low albuminemia	1 (1)	0 (0)	1 (1)	0 (0)	0 (0)	0 (0)	0 (0)	0 (0)	0 (0)
Nausea/anorexia/pain/ascites	4 (2)	2 (2)	6 (2)	0 (0)	0 (0)	0 (0)	0 (0)	0 (0)	0 (0)

therapy would be the best therapeutic option for patients who have tumors that preclude currently available local therapies because of tumor size, macroscopic vascular invasion, or deep tumor location.

According to the BCLC classification, the 5-year overall survival rate of patients in the operable group was 67.6%. This survival rate is comparable to reported data associated with hepatic resection.[21] It is noteworthy that the overall survival rate of patients classified with stage C disease at 5 years was 30.6% in the current study; this is far superior to other reported data.[21] Patients in this stage have macroscopic vascular invasion and/or extrahepatic metastasis. According to the BCLC classification, these patients usually are excluded from curative treatments and receive either TACE or sorafenib. In the current study, most of patients with stage C disease had macroscopic vascular invasion without extrahepatic metastasis. They were received proton and carbon ion therapies with curative intent, and the local control rates for these patients exceeded 80% (Table 4). These results suggest that some of patients with BCLC stage C disease may benefit from more aggressive local therapies, such as particle therapy.

Most of the treatment-related toxicities in the current study were transient, easily managed, and acceptable. Rib fracture and dermatitis were observed frequently in patients who were treated during the early period at our center. Most of these patients, including 1 patient with grade 4 dermatitis, were treated with only 1 portal to obtain an adequate spread-out Bragg peak. Thereafter, we used 2 or more portals and rarely observed such complications. Regarding intrahepatic structure-related complications, no studies, including ours, have reported blood vessel-related complications. This is a distinct advantage of particle therapy over other local therapies and supports our proposal that tumors in perivascular locations are appropriate candidates for particle therapy. In contrast, although less common, bile duct complications, including biloma and stenosis, have been reported in several studies.[16] In the current study, biloma formation was observed in 1 patient whose tumor was adjacent to the porta hepatis. The bile duct may stand as the single greatest obstacle of intrahepatic structures after particle therapy. It is almost impossible to predict bile duct complications before treatment; thus, tumors adjacent to the porta hepatis should be treated with caution.

Grade 2 or greater gastrointestinal ulceration was observed in 5 patients whose tumors were adjacent to the gut. To minimize toxicity in these patients, we reduced the fraction size and initiated proton pump inhibitors immediately after treatment; and, ultimately, we were able to prevent the development of severity. The proximity of the gut is an important consideration in selecting particle therapy for patients with HCC. We introduced operative placement of a spacer between the tumor and the gut before particle therapy as a countermeasure for this limitation to ensure safe irradiation.[37,38]

To our knowledge, this is the first study to assess the clinical treatment results from both proton therapy and carbon ion therapy. However, our study has some important limitations: 1) the results of this study were achieved retrospectively and not through randomized or controlled trials; 2) during the study period, we used different treatment protocols for proton therapy and carbon ion therapy; and 3) the RBE of carbon ion beams for HCC

has not been completely clarified. Although further investigation is required, our data can serve as a basis for future refinement of beam selection.

In conclusion, both proton therapy and carbon ion therapy produce favorable results as treatment for HCC. Both therapies have great advantages in treating HCC, a condition that is a contraindication for other local therapies. Randomized clinical trials are required to compare particle therapy with other local therapies and to clarify the roles played by particle therapy in the HCC treatment algorithm.

FUNDING SOURCES

This study was supported by grants-in aid for Scientific Research from the Ministry of Education, Culture, Sports, Science, and Technology of Japan to Y.H. (C-21591773), Y.K. (C-20591611), and M.M. (B-22390234) and by grants for Global Center of Excellence Program for Education and Research on Signal Transduction Medicine in the Coming Generation "Bringing Up Clinician-Scientists in the Alliance Between Basic and Clinical Medicine" (to Y.K.).

CONFLICT OF INTEREST DISCLOSURES

The authors made no disclosures.

REFERENCES

1. Parkin DM. Global cancer statistics in the year 2000. *Lancet Oncol.* 2001;2:533-543.
2. El-Serag HB, Rudolph KL. Hepatocellular carcinoma: epidemiology and molecular carcinogenesis. *Gastroenterology.* 2007;132:2557-2576.
3. Hasegawa K, Makuuchi M, Takayama T, et al. Surgical resection vs percutaneous ablation for hepatocellular carcinoma: a preliminary report of the Japanese nationwide survey. *J Hepatol.* 2008;49:589-594.
4. Bismuth H, Majno PE, Adam R. Liver transplantation for hepatocellular carcinoma. *Semin Liver Dis.* 1999;19:311-322.
5. Llovet JM, Burroughs A, Bruix J. Hepatocellular carcinoma. *Lancet.* 2003;362:1907-1917.
6. Fan ST, Lo CM, Liu CL, et al. Hepatectomy for hepatocellular carcinoma: toward zero hospital deaths. *Ann Surg.* 1999;229:322-330.
7. Lam VW, Ng KK, Chok KS, et al. Risk factors and prognostic factors of local recurrence after radiofrequency ablation of hepatocellular carcinoma. *J Am Coll Surg.* 2008;207:20-29.
8. Mulier S, Ni Y, Jamart J, Ruers T, Marchal G, Michel L. Local recurrence after hepatic radiofrequency coagulation: multivariate meta-analysis and review of contributing factors. *Ann Surg.* 2005;242:158-171.
9. Berber E, Siperstein A. Local recurrence after laparoscopic radiofrequency ablation of liver tumors: an analysis of 1032 tumors. *Ann Surg Oncol.* 2008;15:2757-2764.
10. Emami B, Lyman J, Brown A, et al. Tolerance of normal tissue to therapeutic irradiation. *Int J Radiat Oncol Biol Phys.* 1991;21:109-122.
11. Lawrence TS, Robertson JM, Anscher MS, Jirtle RL, Ensminger WD, Fajardo LF. Hepatic toxicity resulting from cancer treatment. *Int J Radiat Oncol Biol Phys.* 1995;31:1237-1248.
12. Hawkins MA, Dawson LA. Radiation therapy for hepatocellular carcinoma: from palliation to cure. *Cancer.* 2006;106:1653-1663.
13. Schulz-Ertner D, Tsujii H. Particle radiation therapy using proton and heavier ion beams. *J Clin Oncol.* 2007;25:953-964.
14. Nakayama H, Sugahara S, Tokita M, et al. Proton beam therapy for hepatocellular carcinoma: the University of Tsukuba experience. *Cancer.* 2009;115:5499-5506.
15. Hata M, Tokuuye K, Sugahara S, et al. Proton beam therapy for hepatocellular carcinoma with limited treatment options. *Cancer.* 2006;107:591-598.
16. Chiba T, Tokuuye K, Matsuzaki Y, et al. Proton beam therapy for hepatocellular carcinoma: a retrospective review of 162 patients. *Clin Cancer Res.* 2005;11:3799-3805.
17. Bush DA, Hillebrand DJ, Slater JM, Slater JD. High-dose proton beam radiotherapy of hepatocellular carcinoma: preliminary results of a phase II trial. *Gastroenterology.* 2004;127:S189-S193.
18. Kato H, Tsujii H, Miyamoto T, et al. Results of the first prospective study of carbon ion radiotherapy for hepatocellular carcinoma with liver cirrhosis. *Int J Radiat Oncol Biol Phys.* 2004;59:1468-1476.
19. Kawashima M, Furuse J, Nishio T, et al. Phase II study of radiotherapy employing proton beam for hepatocellular carcinoma. *J Clin Oncol.* 2005;23:1839-1846.
20. Hishikawa Y, Oda Y, Mayahara H, et al. Status of the clinical work at Hyogo. *Radiother Oncol.* 2004;73(suppl 2):S38-S40.
21. Llovet JM, Fuster J, Bruix J. The Barcelona approach: diagnosis, staging, and treatment of hepatocellular carcinoma. *Liver Transpl.* 2004;10:S115-S120.
22. Liver Cancer Study Group of Japan, ed. General Rules for the Clinical and Pathological Study of Primary Liver Cancer. 2nd English ed. Tokyo, Japan: Kanehara; 2003.
23. Nakashima Y, Nakashima O, Tanaka M, Okuda K, Nakashima M, Kojiro M. Portal vein invasion and intrahepatic micrometastasis in small hepatocellular carcinoma by gross type. *Hepatol Res.* 2003;26:142-147.
24. Demizu Y, Murakami M, Miyawaki D, et al. Analysis of vision loss caused by radiation-induced optic neuropathy after particle therapy for head-and-neck and skull-base tumors adjacent to optic nerves. *Int J Radiat Oncol Biol Phys.* 2009;75:1487-1492.
25. Minohara S, Kanai T, Endo M, Noda K, Kanazawa M. Respiratory gated irradiation system for heavy-ion radiotherapy. *Int J Radiat Oncol Biol Phys.* 2000;47:1097-1103.
26. Forner A, Ayuso C, Varela M, et al. Evaluation of tumor response after locoregional therapies in hepatocellular carcinoma: are response evaluation criteria in solid tumors reliable? *Cancer.* 2009;115:616-623.
27. Keppke AL, Salem R, Reddy D, et al. Imaging of hepatocellular carcinoma after treatment with yttrium-90 microspheres. *AJR Am J Roentgenol.* 2007;188:768-775.
28. Mizumoto M, Tokuuye K, Sugahara S, et al. Proton beam therapy for hepatocellular carcinoma adjacent to the porta hepatis. *Int J Radiat Oncol Biol Phys.* 2008;71:462-467.

29. Tse RV, Guha C, Dawson LA. Conformal radiotherapy for hepatocellular carcinoma. *Crit Rev Oncol Hematol.* 2008;67: 113-123.
30. Cheng JC, Wu JK, Huang CM, et al. Dosimetric analysis and comparison of 3-dimensional conformal radiotherapy and intensity-modulated radiation therapy for patients with hepatocellular carcinoma and radiation-induced liver disease. *Int J Radiat Oncol Biol Phys.* 2003;56:229-234.
31. Dawson LA. Protons or photons for hepatocellular carcinoma? Let's move forward together. *Int J Radiat Oncol Biol Phys.* 2009;74:661-663.
32. Suit H, DeLaney T, Goldberg S, et al. Proton vs carbon ion beams in the definitive radiation treatment of cancer patients. *Radiother Oncol.* 2010;95:3-22.
33. International Commission on Radiation Units and Measurements (IRCU). Prescribing, recording, and reporting proton-beam therapy (IRCU Report 78). *J IRCU.* 2007;7: 2-2.
34. Paganetti H, Niemierko A, Ancukiewicz M, et al. Relative biological effectiveness (RBE) values for proton beam therapy. *Int J Radiat Oncol Biol Phys.* 2002;53:407-421.
35. Lu DS, Raman SS, Limanond P, et al. Influence of large peritumoral vessels on outcome of radiofrequency ablation of liver tumors. *J Vasc Interv Radiol.* 2003;14:1267-1274.
36. Lam VW, Ng KK, Chok KS, et al. Incomplete ablation after radiofrequency ablation of hepatocellular carcinoma: analysis of risk factors and prognostic factors. *Ann Surg Oncol.* 2008;15:782-790.
37. Fukumoto T, Komatsu S, Hori Y, Murakami M, Hishikawa Y, Ku Y. Particle beam radiotherapy with a surgical spacer placement for advanced abdominal leiomyosarcoma results in a significant clinical benefit. *J Surg Oncol.* 2010;101:97-99.
38. Komatsu S, Hori Y, Fukumoto T, Murakami M, Hishikawa Y, Ku Y. Surgical spacer placement and proton radiotherapy for unresectable hepatocellular carcinoma. *World J Gastroenterol.* 2010;16:1800-1803.

An extremely rare portal annular pancreas for pancreaticoduodenectomy with a special note on the pancreatic duct management in the dorsal pancreas

Ippei Matsumoto, MD, PhD, Makoto Shinzeki, MD, PhD, Takumi Fukumoto, MD, PhD, *and* **Yonson Ku, MD, PhD,** *Kobe, Japan*

From the Division of Hepato-Biliary-Pancreatic Surgery, Department of Surgery, Kobe University Graduate School of Medicine, Chuo-Ku, Kobe, Japan

A PREVIOUSLY HEALTHY 81-YEAR-OLD WOMAN with general fatigue was admitted to our hospital in June 2009. Her blood chemistry data were within normal limits except for slightly elevated liver function values. Serum levels of carbohydrate antigen 19-9 and carcinoembryonic antigen were both normal. Gastroduodenoscopy showed an erosive tumor in the ampulla of Vater. Dynamic computed tomography (CT) revealed bilateral intrahepatic biliary dilatation, and the superior mesenteric vein (SMV) circumferentially embedded in the body of the pancreas, as well as a slightly dilated main pancreatic duct (MPD) in the tissue behind the SMV (Fig 1). The MPD was found posteriorly to the SMV and the accessory pancreatic duct (APD) was seen anteriorly to the SMV. The 2 ducts joined in the body of the pancreas to the left side of the SMV. A preoperative diagnosis was cancer of the ampulla of Vater accompanying a portal annular pancreas (PAP). The patient underwent pancreaticoduodenectomy (PD). Intraoperatively, after transection of the pancreas on the SMV, we saw the parenchyma of the uncinate process communicating behind the SMV with the body of the pancreas (Fig 2, *A*). We inserted a small tube into the cut orifice of the distal APD and performed intraoperative pancreatography. The dilated MPD and the point of the ductal conjunction were confirmed (Fig 2, *B* and *C*). Pancreaticojejunostomy was performed after a second pancreatic transection at the distal side of the ductal conjunction. Histologically, the resected specimen revealed an adenocarcinoma of the ampulla of Vater. The postoperative course was uneventful and the patient was discharged on postoperative day 32.

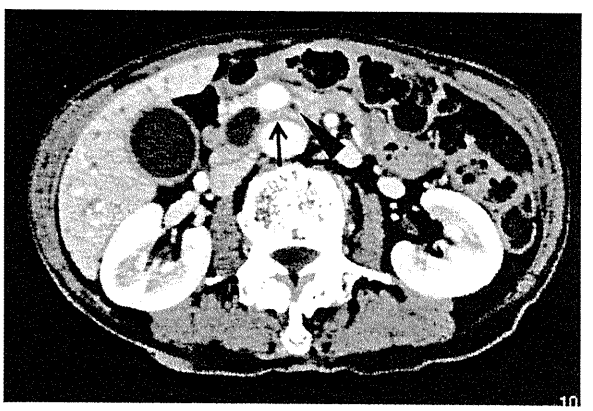

Fig 1. Dynamic CT imaging showing pancreatic tissue completely encircling the superior mesenteric vein (SMV; *arrow*) and a dilated main pancreatic duct in the tissue behind the SMV (*arrow head*).

DISCUSSION

PAP is a rare pancreatic anomaly in which the uncinate process of the pancreas extends to and is fused to the dorsal surface of the body of the pancreas by surrounding the portal vein or the SMV. During pancreatic surgery, the presence of PAP significantly affects the procedure, especially pancreatico-intestinal reconstruction after PD. Although an incidence of 1.14% has been reported by Karasaki et al,[1] based on an institutional review of CT scans, only 11 cases of PAP have been reported in the English literature.[2] Four of these cases had

Accepted for publication August 16, 2011.

Reprint requests: Ippei Matsumoto, MD, PhD, Division of Hepato-Biliary-Pancreatic Surgery, Department of Surgery, Kobe University Graduate School of Medicine, 7-5-2 Kusunoki-Cho Chuo-Ku Kobe, 650-0017 Japan. E-mail: imatsu@med.kobe-u.ac.jp.

Surgery 2011;■:■-■.

0039-6060/$ - see front matter

doi:10.1016/j.surg.2011.08.017

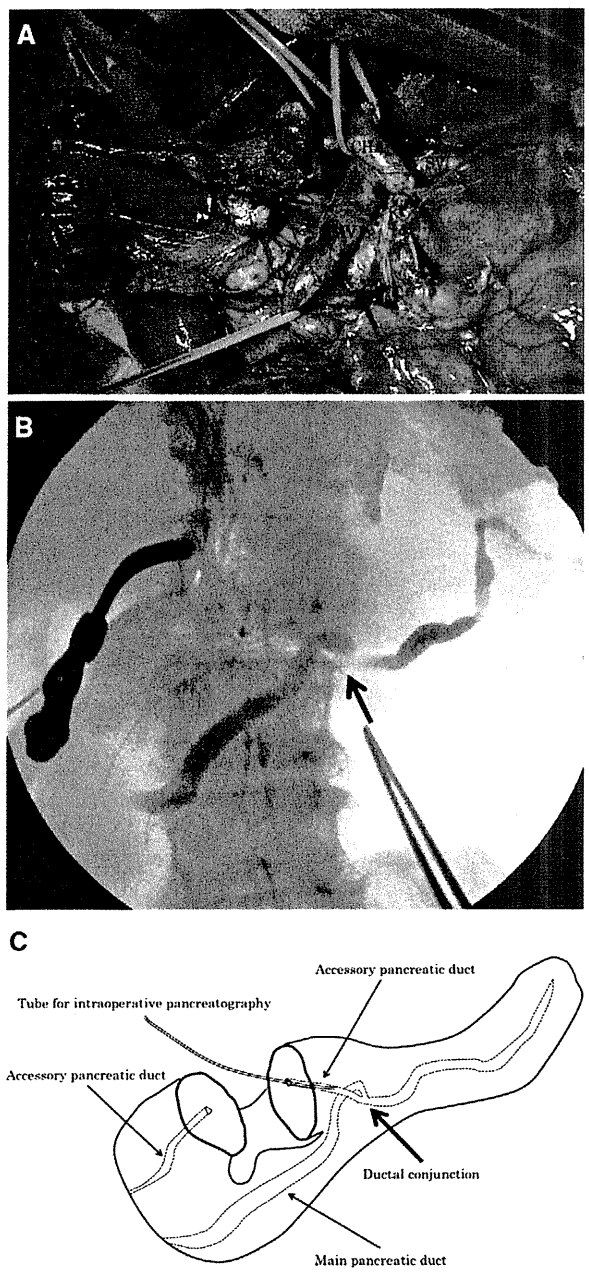

Fig 2. *A*, Intraoperative findings. The parenchyma of the uncinate process is communicating behind the superior mesenteric vein (SMV) with the body of the pancreas (*arrow*), as seen after transecting the pancreas on the SMV. A small tube was inserted into the cut orifice of the distal accessory pancreatic duct (*arrow head*) to perform intraoperative pancreatography. *CHA*, Common hepatic artery; *SV*, splenic vein. *B*, Intraoperative pancreatography showing a dilated main pancreatic duct and the point of the ductal conjunction (*arrow*). *C*, Scheme of the intraoperative pancreatography.

PD performed due to periampullary disease.[1-4] Joseph et al[2] reviewed all 11 cases and proposed a new classification according to their positioning of the MPD: Type I, when the ventral bud of the pancreas is fused to the body with the MPD posterior to the PV without the APD; type II, when type I is associated with pancreas divisum; and type III, when the uncinate process without the ductal system is involved in the encasement of the PV and fusion. Therefore, to our knowledge, this is the first case showing the MPD posterior to the SMV and APD anterior to the SMV and the 2 ducts joining in the body of the pancreas.

Pancreatico-intestinal reconstruction is an important procedure to prevent postoperative pancreatic fistula (POPF), which is associated with prolonged hospital stay, intra-abdominal abscess and hemorrhage. Marjanovic et al[4] reported a case of PD with a modification of the resection of the pancreatic head accompanying PAP for a duodenal-infiltrating gastric cancer. This patient's postoperative course was complicated by accumulation of fluid related to the POPF. To simplify pancreatico-intestinal reconstruction and reduce the risk of POPF, we transected the pancreas at the distal side of the ductal conjunction. Intraoperative pancreatography was useful for confirmation of the structure of the ductal system and deciding the position of pancreas transection.

In conclusion, we report a case of PAP, which is an extremely rare pancreatic anomaly. It is very important to confirm pancreatic ductal system integrity preoperatively and intraoperatively when recognizing this anomaly to avoid technical problems at the time of PD.

REFERENCES

1. Karasaki H, Mizukami Y, Ishizaki A, Goto J, Yoshikawa D, Kino S, et al. Portal annular pancreas, a notable pancreatic malformation: frequency, morphology, and implications for pancreatic surgery. Surgery 2009;146:515-8.
2. Joseph P, Raju RS, Vyas FL, Eapen A, Sitaram V. Portal annular pancreas. A rare variant and a new classification. JOP 2010;11:453-5.
3. Sugiura Y, Shima S, Yonekawa H, Yoshizumi Y, Ohtsuka H, Ogata T. The hypertrophic uncinate process of the pancreas wrapping the superior mesenteric vein and artery: a case report. Jpn J Surg 1987;17:182-5.
4. Marjanovic G, Obermaier R, Benz S, Bley T, Juettner E, Hopt UT, et al. Complete pancreatic encasement of the portal vein: surgical implications of an extremely rare anomaly. Langenbecks Arch Surg 2007;392:489-91.

J Gastrointest Surg (2011) 15:2296–2298
DOI 10.1007/s11605-011-1543-5

GI IMAGE

A Focal Mass-Forming Autoimmune Pancreatitis Mimicking Pancreatic Cancer with Obstruction of the Main Pancreatic Duct

Ippei Matsumoto · Makoto Shinzeki · Hirochika Toyama · Sadaki Asari · Tadahiro Goto · Isamu Yamada · Tetsuo Ajiki · Takumi Fukumoto · Yonson Ku

Received: 22 March 2011 / Accepted: 5 April 2011 / Published online: 17 May 2011

Abstract
Introduction and background Autoimmune pancreatitis (AIP) is a rare disease that closely mimics pancreatic cancer (PC) in its presentation. It is very important for clinicians to distinguish one from the other because their treatment and prognosis are vastly different. Typical radiological imaging findings, in particular observation of diffusely or segmentally narrowed main pancreatic duct (MPD) with an irregular wall by endoscopic retrograde cholangiopancreatography (ERCP), are essential for making the diagnosis of AIP. On the other hand, MPD obstruction is one of the most frequent features on ERCP.
Case report We report a rare case of a patient with focal mass-forming AIP strongly suspected of being PC because of MPD obstruction on ERCP.
Conclusion It was difficult to distinguish PC from AIP with current diagnostic modalities. We will continue to make an effort to distinguish between the two disorders to prevent unnecessary surgery.

Keywords Autoimmune pancreatitis · Pancreatic cancer · Endoscopic retrograde cholangiopancreatography · Main pancreatic duct · Diagnosis

Autoimmune pancreatitis (AIP) is a rare disease that closely mimics pancreatic cancer (PC) in its presentation. It is very important for clinicians to distinguish one from the other because their treatment and prognosis are vastly different. In 2006, the Japanese Pancreas Society proposed clinical diagnostic criteria for AIP based on a combination of clinical, laboratory, imaging, and histological findings.[1] According to these criteria, typical radiological imaging findings, in particular observation of diffusely or segmentally narrowed main pancreatic duct (MPD) with an irregular wall by endoscopic retrograde cholangiopancreatography (ERCP), are essential for making the diagnosis of AIP. On the other hand, MPD obstruction is one of the most frequent features on ERCP.

Here, we report a rare case of a patient with focal mass-forming (FMF) AIP strongly suspected of being PC because of MPD obstruction on ERCP.

Case Report

A previously healthy 79-year-old man with epigastric pain was admitted to another hospital. After examination, he was diagnosed as having acute pancreatitis due to a tumor of the pancreatic tail. After treatment for pancreatitis, he was referred to our hospital for further examination and treatment of the tumor. The patient's blood chemistry data were within normal limits except for slightly elevated serum pancreatic amylase (264 IU/l) and lipase levels (430 IU/l). Serum levels of CA19-9 and CEA were both normal. Serum gamma globulin and total IgG were normal, but IgG4 was elevated (256 mg/dl). Serum autoantibodies and rheumatoid factor were negative. Dynamic CT imaging revealed an irregular mass measuring 40×23 mm in the tail of the pancreas. The tumor was not enhanced on the arterial phase and slightly enhanced on the portal phase (Fig. 1a).

I. Matsumoto (✉) · M. Shinzeki · H. Toyama · S. Asari · T. Goto · I. Yamada · T. Ajiki · T. Fukumoto · Y. Ku
Division of Hepato-Biliary-Pancreatic Surgery, Department of Surgery, Kobe University Graduate School of Medicine, 7-5-2 Kusunoki-Cho, Chuo-Ku, Kobe 650-0017, Japan
e-mail: imatsu@med.kobe-u.ac.jp

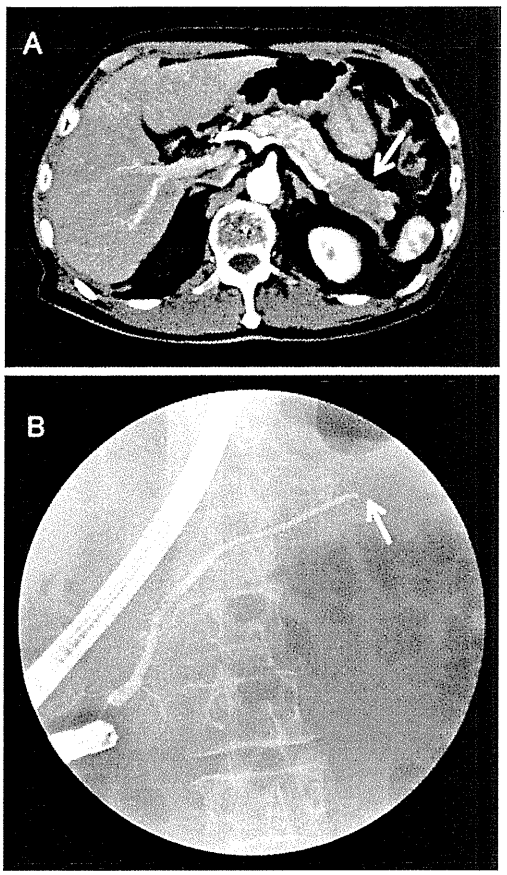

Fig. 1 Dynamic abdominal CT scans in arterial phase showed a low-density mass (*arrow*) measuring 40×23 mm in the tail of the pancreas (**a**). ERCP showed an obstruction of the MPD (*arrow*) at the site of the pancreatic mass (**b**)

The splenic vein was obstructed by the tumor. MRI imaging showed that the intensity decreased in the T1-weighted images of the pancreas and increased in the T2-weighted images. Endoscopic ultrasonography (EUS) revealed a hypoechoic lesion detected in the tail of the pancreas. EUS-guided fine needle aspiration (EUS-FNA), however, did not reveal any cancer cells. 18-Fluorodeoxyglucose positron emission tomography (FDG-PET) showed hot spots of FDG uptake at the site of the pancreatic mass. No extrapancreatic lesions were detected. ERCP revealed an obstruction of the MPD at the site of the tumor (Fig. 1b). Insertion of a guidewire to the distal MPD was impossible. Brush cytology was negative for cancer cells. We suspected PC concomitant with AIP or rather than AIP. The patient underwent a distal pancreatectomy with an uneventful postoperative course.

Gross inspection of the resected specimen revealed a diffusely enlarged and firm pancreas. Histologically, it was remarkable for an intense mixed inflammatory cell infiltrate predominantly composed of lymphocytes and plasma cells, and centered on the pancreatic ducts. The inflammation was associated with significant acinar dropout and parenchymal fibrosis. An obliterative venulitis was noted at the leading edges of the inflammatory cell infiltrate. Immunohistochemical labeling with an antibody to IgG4 revealed large numbers of IgG4-expressing plasma cells.

Discussion

Although diagnosis of AIP has improved thanks to a growing awareness of the condition and proposed diagnostic criteria,[1] there remains no practical strategy to differentiate PC from AIP. One must distinguish between the two disorders to prevent unnecessary surgery or delayed initiation of corticosteroid therapy. However, about 3–5% of patients undergoing pancreatic resection for presumed PC in fact has AIP.[2] Kamisawa et al.[3] reported that 7 of 37 (18.9%) AIP patients had surgery because they were misdiagnosed as having PC or bile duct cancer. In particular, it is very difficult to differentiate between FMF AIP and PC. Chang et al.[4] reported that 8 of 26 (31.8%) AIP patients were FMF AIP who were frequently surgically treated because differentiating FMF AIP from PC was so difficult. Kamisawa et al.[3] also reported that 6 of 17 (35.3%) FMF AIP patients were surgically treated (resection; 3, bypass operation; 3) because PC was suspected.

To obtain images of the pancreatic duct, it is necessary to use ERCP, and additionally direct images taken during the operation or of specimens. Kamisawa et al.[3] reported that the three ERCP features required for AIP diagnosis were (1) a >3-cm-long narrowed main pancreatic duct; (2) skip lesion of the MPD; and (3) maximal upstream MPD diameter of <5 mm. On the other hand, features highly suggestive of PC were a pancreatic low density mass, MPD obstruction, distal pancreatic atrophy, and metastases. There have been four reports of retrospective evaluation of ERCP imaging in AIP patient.[3,5–7] The frequency of MPD obstruction on ERCP in AIP patients was 0–5.9%, whereas in PC patients, it was 35–60%, but only three patients with MPD obstruction have been reported. Although the measurement of serum IgG4 level is useful for differentiating between the two diseases, 10% of PC patients also has elevated IgG4.[8] Moreover, there are a few reports of AIP patients with concomitant PC.[9,10] EUS-FNA is frequently used to rule out PC. However, its accuracy for PC is not perfect (about 70–90%) because some cases of PC are accompanied by chronic inflammation and fibrosis around the mass, so a negative biopsy does not rule out cancer. Diagnosis of AIP by EUS-FNA is difficult because the specimen is too small. Taken together, we cannot exclude the presence of PC in many cases. Further improvement of diagnostic strategies, such as core biopsy techniques, or development of new immunohistological diagnostic criteria from results of cytologic and tissue specimen analyses are needed to avoid unnecessary surgery.

In conclusion, we report an extremely rare case of FMF AIP mimicking PC with MPD obstruction. It was difficult to distinguish PC from AIP with current diagnostic modalities.

References

1. Okazaki K, Kawa S, Kamisawa T et al. Clinical diagnostic criteria of autoimmune pancreatitis: revised proposal. J Gastroenterol 2006; 41: 626–631.
2. Wolfson D, Barkin JS, Chari ST et al. Management of pancreatic masses. Pancreas 2005; 31: 203–217.
3. Kamisawa T, Imai M, Yui Chen P et al. Strategy for differentiating autoimmune pancreatitis from pancreatic cancer. Pancreas 2008; 37: e62–67
4. Chang WI, Kim BJ, Lee JK et al. The clinical and radiological characteristics of focal mass-forming autoimmune pancreatitis: comparison with chronic pancreatitis and pancreatic cancer. Pancreas 2009; 38: 401–408.
5. Horiuchi A, Kawa S, Hamano H et al. ERCP features in 27 patients with autoimmune pancreatitis. Gastrointest Endosc 2002; 55: 494–499.
6. Wakabayashi T, Kawaura Y, Satomura Y et al. Clinical and imaging features of autoimmune pancreatitis with focal pancreatic swelling or mass formation: comparison with so-called tumor-forming pancreatitis and pancreatic carcinoma. Am J Gastroenterol 2003; 98: 2679–2687.
7. Nishino T, Oyama H, Toki F, Shiratori K. Differentiation between autoimmune pancreatitis and pancreatic carcinoma based on endoscopic retrograde cholangiopancreatography findings. J Gastroenterol 2010; 45: 988–996.
8. Ghazale A, Chari ST, Smyrk TC et al. Value of serum IgG4 in the diagnosis of autoimmune pancreatitis and in distinguishing it from pancreatic cancer. The American journal of gastroenterology 2007; 102: 1646–1653.
9. Inoue H, Miyatani H, Sawada Y, Yoshida Y. A case of pancreas cancer with autoimmune pancreatitis. Pancreas 2006; 33: 208–209.
10. Witkiewicz AK, Kennedy EP, Kennyon L et al. Synchronous autoimmune pancreatitis and infiltrating pancreatic ductal adenocarcinoma: case report and review of the literature. Hum Pathol 2008; 39: 1548–1551.

Hepatocellular carcinomas can develop in simple fatty livers in the setting of oxidative stress

Sir,

It is doubtless that non-alcoholic fatty liver disease (NAFLD) has become a critical public health issue in most developed countries.[1] In addition to its close association with metabolic disorders and cardiovascular events, NAFLD itself can progress to life-threatening liver diseases, cirrhosis and hepatocellular carcinoma (HCC).[1,2] Surprisingly, recent clinical observations have revealed that HCC can develop in non-cirrhotic, but steatotic livers without significant fibrosis.[3,4] In the reports, authors emphasised the importance of underlying metabolic disorders and oxidative stress in hepatocarcinogenesis in such NAFLD cases.

We herein report a case of NAFLD complicated by HCC, in which the potential contribution of oxidative stress to hepatocarcinogenesis in NAFLD has been further strongly suggested.

In May 2006, a 72-year-old obese Japanese man was admitted to the National Hospital Organization Osaka National Hospital, Japan, because of a hepatic nodule. The patient had a 5 year medical history of hypertension and fatty liver. He underwent an operation for abdominal aortic aneurysm in April 2004, and had since been an outpatient. Follow-up abdominal ultrasonography showed, in addition to hepatic steatosis, a nodular lesion approximately 2 cm in diameter in the left lobe of the liver. The hepatic nodule had been growing larger, and findings of computed tomography (CT) strongly suggested that it was HCC (Fig. 1).

On admission, he appeared to be healthy except for obesity, and the laboratory test results showed normal serum levels of transaminases and negativity for hepatitis B and C viruses. After the examinations, under the tentative diagnosis of HCC, a surgical operation was performed to remove the left lobe of the liver. The cut surface of the liver sample was smooth and yellowish-brown, and demonstrated the clearly circumscribed nodule 5 cm in diameter (Fig. 2). Histological examination revealed that the nodular lesion was well-differentiated HCC (Fig. 3A), and the background hepatic disorder was simple steatosis without inflammation and fibrosis (Fig. 3B). Routine pathological examination couldn't detect any causative factors in hepatocarcinogenesis, such as iron overload. However, an immunohistochemical analysis revealed that as well as tumour cells, a few non-tumourous hepatocytes showed immunoreactivity for anti-oxidised phosphatidylcholine (oxPC; Fig. 3A,B insets), a marker of

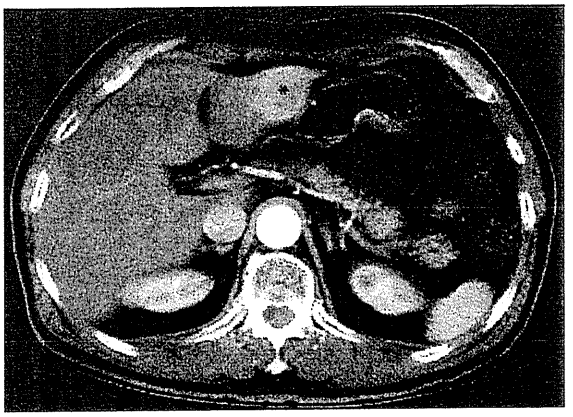

Fig. 1 Findings of computed tomography. A hypervascular nodule is seen in the left lobe of the liver (asterisk).

Fig. 2 The cut-surface of the liver sample. A well-circumscribed nodular lesion 5 cm in diameter is present.

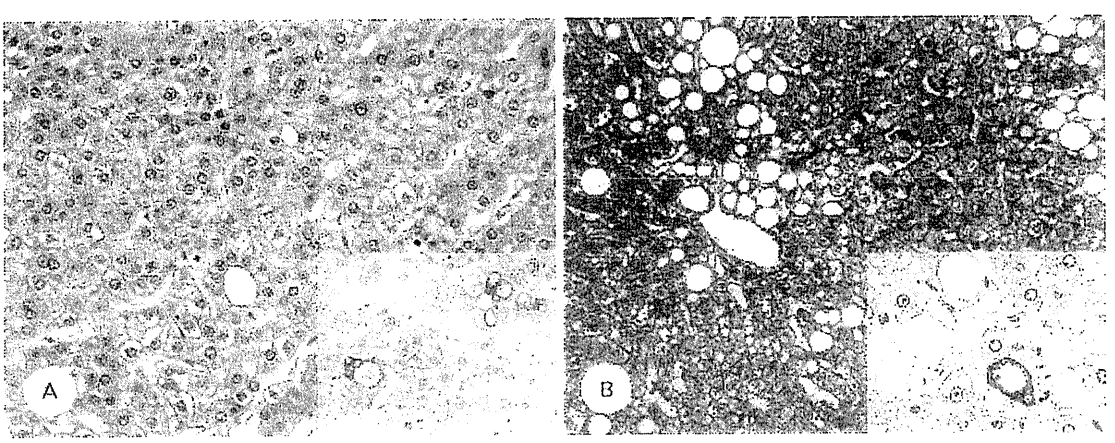

Fig. 3 Microscopic findings of the liver sample. (A) The hepatic nodule consists of well-differentiated HCC (H&E). (B) A background liver condition is simple steatosis without fibrosis (Azan-Mallory stain for collagen). Insets: steatotic liver cells of both tumourous and non-tumourous portions are positive for oxPC (immunoperoxidase with anti-oxPC).

oxidative cellular injury.[5] The immunoreactivity was found restrictively in steatotic cells in both tumourous and non-tumourous portions. It suggested that the steatosis-related oxidative hepatocellular injury had persisted and had played a certain role in the development of HCC. His postoperative course was uneventful and he was discharged. Follow-up examinations have been done every 3 months, resulting in no evidence of tumour recurrence. When last seen, in December 2009, he was well.

Like the present case, HCC can develop in non-inflammatory, non-fibrotic, but steatotic livers. A previous case report of HCC arising in the absence of advanced NAFLD emphasised the potential roles for metabolic factors (diabetes, hypertension, obesity and dyslipidaemia) and oxidative stress in hepatocarcinogenesis.[4] Oxidative stress is generally recognised as an important factor in hepatocarcinogenesis.[2,6] Our immunohistochemical results showed oxPC-positive steatotic hepatocytes in the background liver tissue of HCC. OxPC, one of the lipid peroxides, is a highly specific marker of oxidative damage. In our previous observation, its immunoreactivity was seen mainly in steatotic or degenerated hepatocytes in NAFLD, and only in some Kupffer cells in normal liver tissues.[5] Hence, the present result suggested that the fatty liver had chronically been exposed to oxidative stress, which was probably initiated prior to hepatocarcinogenesis. To our knowledge, this is the first direct evidence of oxidative hepatocellular injury occurring in simple fatty livers complicated by HCC. Excess fat accumulation itself, even in the absence of inflammation, can be a source of oxidative stress that induces hepatocarcinogenesis. In conclusion, simple steatosis-related oxidative stress should be considered as one of the risk factors of HCC.

Yoshihiro Ikura*
Eiji Mita†
Shoji Nakamori‡

**Department of Pathology, Osaka City University Graduate School of Medicine, Osaka, †Departments of Gastroenterology, and ‡Surgery, National Hospital Organization, Osaka National Hospital, Osaka, Japan*

Contact Dr Y. Ikura.
E-mail: ikura@med.osaka-cu.ac.jp

1. Neuschwander-Tetri BA, Caldwell SH. Nonalcoholic steatohepatitis: summary of an AASLD Single Topic Conference. *Hepatology* 2003; 37: 1202–19.
2. Caldwell SH, Crespo DM, Kang HS, Al-Osaimi AM. Obesity and hepatocellular carcinoma. *Gastroenterology* 2004; 127(Suppl 1): S97–103.
3. Paradis V, Zalinski S, Chelbi E, Guedj N, Degos F, Vilgrain V, *et al.* Hepatocellular carcinomas in patients with metabolic syndrome often develop without significant liver fibrosis: a pathological analysis. *Hepatology* 2009; 49: 851–9.
4. Guzman G, Brunt EM, Petrovic LM, Chejfec G, Layden TJ, Cotler SJ. Does nonalcoholic fatty liver disease predispose patients to hepatocellular carcinoma in the absence of cirrhosis? *Arch Pathol Lab Med* 2008; 132: 1761–6.
5. Ikura Y, Ohsawa M, Suekane T, *et al.* Localization of oxidized phosphatidylcholine in nonalcoholic fatty liver disease: impact on disease progression. *Hepatology* 2006; 43: 506–14.
6. Sasaki Y. Does oxidative stress participate in the development of hepatocellular carcinoma? *J Gastroenterol* 2006; 41: 1135–48.

DOI: 10.1097/PAT.0b013e32834274ec

Benign prostatic glands as a tissue component of testicular teratoma: an uncommon histological finding

Sir,

The occurrence of benign prostatic tissue as a component of testicular teratoma has only been described as a single case report.[1] This may be due to its rare occurrence, as well as the failure of the diagnostic pathologist to recognise glands as prostatic on routine sections and to subsequently confirm this by immunohistochemistry. In our laboratory we utilise Solufix (Tissugen, Australia), a glutaraldehyde-based tissue fixative for routine histology. This agent preserves the spermine content of prostatic secretory granules (PSG) which stain intensely with eosin on routine stains allowing easy recognition of prostatic epithelium.[2]

We present two cases of benign prostatic glandular tissue occurring in two patients with primary testicular tumours; a mature teratoma in a 35-year-old male and a mixed germ cell tumour (30% mature teratoma) in a 39-year-old male. Each patient underwent routine inguinal orchidectomy for a clinically detected testicular mass.

On microscopy, benign gland structures were recognised which were lined by two cell types and bore some resemblance to prostatic acini. These glands were highlighted by their intense eosinophilic PSG (Fig. 1 and 2), and were distributed either singularly or as clusters separated by bland stroma. Lining epithelium showed variable morphology ranging from bland epithelial cells consistent with benign prostatic glands (Fig. 1) to epithelial cells with larger nuclei and prominent nucleoli (Fig. 2), consistent with prostatic intraepithelial neoplasia (PIN). The prostatic nature of the glands was subsequently confirmed by strong diffuse cytoplasmic reactivity with immunohistochemistry for PSA (Dako, USA; Fig. 1 inset) and prostatic acid phosphatase (Dako; not shown). Basal cells were confirmed with immunostaining for high molecular weight cytokeratin 34βE12 (Dako; Fig. 2 inset).

Recognition of the first case prompted a histological review of all testicular teratomas over a 10 year period which included 20 testicular tumours comprising pure teratomas ($n = 10$) and mixed germ cell tumours with a mature teratoma component of $>10\%$ ($n = 10$). This review identified the second case,

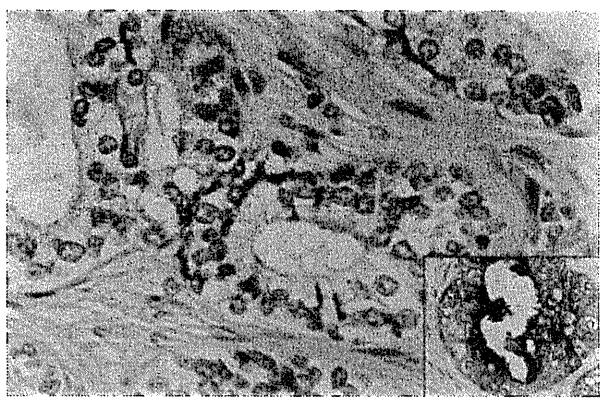

Fig. 1 Benign prostatic glands within a testicular germ cell tumour surrounded by bland stroma. Small eosinophilic granules (prostate secretory granules) are seen in the apical cytoplasm confirming prostatic epithelial differentiation. Inset: These cells are strongly labelled with PSA immunostaining.

Cancer Chemother Pharmacol
DOI 10.1007/s00280-010-1371-4

ORIGINAL ARTICLE

Predictive factors for the effectiveness of neoadjuvant chemotherapy and prognosis in triple-negative breast cancer patients

Hiroko Masuda · Norikazu Masuda · Yoshinori Kodama · Masami Ogawa · Michiko Karita · Jun Yamamura · Kazunori Tsukuda · Hiroyoshi Doihara · Shinichiro Miyoshi · Masayuki Mano · Shoji Nakamori · Toshimasa Tsujinaka

Received: 24 January 2010 / Accepted: 14 May 2010

Abstract
Purpose Triple-negative breast cancers (TNBCs) do not derive benefit from molecular-targeted treatments such as endocrine therapy or anti-HER2 therapy because they lack those molecular targets. On the other hand, TNBCs have been shown to respond to neoadjuvant chemotherapy (NAC). In this study, we analyzed TNBC patients who were treated with NAC at Osaka National Hospital over a recent 5-year period to clarify the predictive factors for NAC and prognostic factors.
Patients and methods Thirty-three TNBC patients underwent sequential NAC with anthracycline (FEC100: 5FU 500 mg/m^2, epirubicin 100 mg/m^2, and cyclophosphamide 500 mg/m^2/q3w, 4 courses) and taxanes (paclitaxel 80 mg/m^2/qw, 12 courses or docetaxel 75 mg/m^2/q3w, 4 courses) from May 2003 to July 2008. Pre-therapeutical and surgical specimens were studied for expressions of ER, PgR, HER-2, EGFR, cytokeratin 5/6, Ki-67, p53 and androgen receptor by immunohistochemistry (IHC). We analyzed clinicopathological factors and molecular markers in regard to the response to NAC and prognosis.
Results Pathological complete response (pCR) was achieved in 12 TNBC patients (36%). The pCR rate in the basal-like phenotype was significantly lower than in the non-basal-like phenotype (23 vs. 64%, respectively: $P = 0.02$). High pre-operative expressions of Ki-67 (≥50%) and HER-2 (2+) were considered as predictive factors for a better response from NAC. Pre-operative Ki-67 expression showed a significant correlation with disease-free survival (DFS) and a lower expression of Ki-67 (<50%) after NAC was favorable for DFS among non-pCR patients.
Conclusions A non-basal-like phenotype and higher expressions of Ki-67 and HER-2 (2+) were favorable factors for NAC. However, a higher expression of Ki-67 on the surgical specimen after NAC was also a poor prognostic factor.

Keywords Triple-negative breast cancer · Neoadjuvant chemotherapy · Pathological complete response · Ki-67 · Basal-like phenotype

Abbreviations

TNBC	Triple negative breast cancer
NAC	Neoadjuvant chemotherapy
pCR	Pathological complete response
ER	Estrogen receptor
PgR	Progesterone receptor
AR	Androgen receptor
EGFR	Epidermal growth factor receptor
CK	Cytokeratin

H. Masuda · N. Masuda · M. Ogawa · M. Karita · J. Yamamura · S. Nakamori · T. Tsujinaka
Department of Surgery,
National Hospital Organization Osaka National Hospital,
Osaka, Japan

Y. Kodama · M. Mano
Department of Pathology,
National Hospital Organization Osaka National Hospital,
Osaka, Japan

H. Masuda (✉) · K. Tsukuda · H. Doihara · S. Miyoshi
Department of Cancer and Thoracic Surgery,
Okayama University Graduate School of Medicine,
Dentistry and Pharmaceutical Sciences,
2-5-1 Shikatacho Kitaku,
Okayama 700-8558, Japan
e-mail: masuhiro123@hotmail.com

Published online: 01 July 2010

Introduction

Triple-negative breast cancers (TNBCs) are characterized by the lack of expression of estrogen receptor (ER), progesterone receptor (PR), and human epidermal growth factor receptor 2 (HER-2). These cancers occur in ~20–25% of all breast cancers and are associated with an unfavorable prognosis. They derive no benefit from molecularly targeted treatments such as endocrine therapy or trastuzumab [1]. Therefore, identifying appropriate treatments for TNBC is an important issue.

Recent precise gene expression analysis revealed that TNBC is a heterogeneous group of tumors. One of the subgroups is a basal-like subtype, which is characterized by similar gene expression as the basal/myoepithelial cells of the normal breast [1–5]. Basal-like breast cancer has also been identified with immunohistochemical (IHC) staining of basal markers, such as cytokeratins (CKs) and epithelial growth factor receptor (EGFR). TNBCs without these basal markers are classified as non-basal-like subtypes, which are rare breast cancers, and classifications based on gene expression have not been clarified yet. Non-basal-like tumors are also reported to have a better prognosis than basal-like phenotypes [6, 7]. Because of the lack of targeted therapies and their aggressive clinical behaviors, TNBCs are relevant groups to be investigated for their characteristics. Though TNBCs are considered to have poor prognosis generally, TNBCs have been shown to be chemosensitive.

Neoadjuvant chemotherapy (NAC) in primary breast cancers has been shown to produce an outcome equivalent to that of adjuvant chemotherapy [8, 9]. Patients who show a pathological complete response (pCR) in the primary tumors after NAC have a better prognosis [10]. The pathological responses are important prognostic parameters and can be used as surrogate parameters for clinical outcome, so we analyzed the effects of clinicopathological factors as well as immunohistochemical factors on pathological responses after NAC. However, the paradox that TNBC and HER-2 positive subtypes showed higher chemosensitivity but worse survival due to higher relapse after chemotherapy is also known well [10, 11].

Several biological markers have been proposed as prognostic characteristics in breast cancers. ER, PR and HER-2 are such biological markers as well as being therapeutic markers and Ki-67, p53 and androgen receptor (AR) are shown to be associated with prognosis [12–16]. AR is known to be present in the majority of primary and metastatic invasive breast tumors and is often co-expressed with ER and PR in these tumors. Though little is known about the role of AR in hormonal response, AR expression has been shown to be associated with a better outcome for untreated breast cancer patients [14]. Ki-67 is a nuclear antigen expressed in the G1, S, and G2 phases but not in the G0 or resting phase of the cell cycle. Ki-67 has been established as a proliferation marker in breast cancers and high proliferation activity has been found to have predictive value for the response to NAC [17]. Also p53 expression status has been used as a predictive factor for response to systemic therapy, because tumor cells with non-functional p53 do not respond to systemic therapy due to a failure in apoptosis [13, 15].

Because chemotherapy is the only treatment other than surgery for TNBC, the definition of clinical markers in regard to chemotherapeutic response and prognosis is very important. However, there are still few studies focusing on TNBC. In this study, we analyzed clinicopathological factors, phenotypes, and molecular markers of TNBC in regard to the response to NAC and prognosis.

Patients and methods

Patients and neoadjuvant chemotherapy

One hundred and 63 breast cancer patients underwent NAC with a sequential regimen containing anthracycline (FEC100: 5FU 500 mg/m^2, epirubicin 100 mg/m^2, cyclophosphamide 500 mg/m^2/q3w, 4 courses) and taxanes (paclitaxel 80 mg/m^2/qw, 12 courses or docetaxel 75 mg/m^2/q3w, 4 courses) at Osaka National Hospital (Osaka, Japan) from May 2003 to July 2008. The criteria for entry were invasive breast cancer patients from 20 to 70 years old with any T and N0-2 disease, who were diagnosed histologically, were absent from distant metastasis and with normal organ functions. Thirty-three patients (20%) among 163 breast cancer patients were identified as TNBCs. The clinical evaluation of the response to NAC was determined by clinical findings, CT and MRI examinations according to RECIST. All patients were included in clinical trials approved by an institutional review board and asked for written informed consent.

Immunohistochemistry

Pre-therapeutical specimens were obtained by the 14G-needle biopsy in all cases and pathological examinations using standard hematoxylin and eosin staining were carried out. Immunohistochemical evaluation for ER, PgR, HER-2, EGFR, CK5/6, Ki-67, p53 and AR in tissue sections were detected using antibodies (ER:Cat.No. 760-2596I, PgR: 760-2816, HER-2:760-2901, EGFR:790-2988, CK5/6:960-4253, Ki-67:760-2910, p53:760-2912, Ventana Japan, Yokohama, Japan, AR:M3562, Dako Japan, Tokyo, Japan). Visualization of the bound antibodies was performed using a DAKO EnvisionTM + System (Dako Japan Inc., Tokyo, Japan) according to the manufacturer's instructions. Positive

cell rates (%) of ER and PgR were determined as a ratio of positive cells to total cancer cells and a value of 10% or higher were rated as positive [18, 19]. HER-2 expression was defined as (0) to (3+) based on positive cell rates and the intensity of IHC staining. Tumors showing weak overexpression (2+) of HER-2 were also tested by the fluorescence in situ hybridization (FISH) method to clarify the gene amplification of the *HER-2* gene. The *HER-2* gene is visualized as green fluorescent grains and a control of centromere 17 is visualized as orange fluorescent grains (Path Vysion, Abbott, IL, USA). Thus, HER-2 positives were either strong positives (3+) from IHC or positive for gene amplification from FISH analysis.

TNBCs are negative for ER, PgR and HER-2 as described earlier. Among TNBCs with 1–9% of ER and/or PgR expression were defined as hormone receptor (HR) weak and analyzed separately. TNBCs with HER-2 (2+) and that were FISH negative were also analyzed separately.

Proliferative activity was determined by IHC for the Ki-67 antibody. Ki-67 values were expressed as the percentage of positive cell counts among at least 100 tumor cells in each case. Patients with positive staining of Ki-67 at 50% or more were defined as high Ki-67 patients. AR and p53 were defined as positive if tumor cells showed positive staining regardless of rate. Basal-like subtype was defined as CK5/6 positive and/or EGFR positive in 5% or more cells.

Surgical treatment

All patients underwent surgical treatment after NAC. Breast conservative therapy or a mastectomy with or without axillary dissection was performed according to the decision of the surgeons' conference. Surgical specimens were histologically analyzed again, and the pathological response for NAC was evaluated. When no residual invasive tumor cells were found, tumors were identified as pathological complete response (pCR). Surgical specimens from non-pCR patients were analyzed for expressions of Ki-67, p53 and AR as described earlier.

Statistics

A univariate analysis of the pCR rate was carried out by the χ^2 test, and a multivariate analysis was done by multiple logistic regression analysis. The patients' survival was calculated from the first date of treatment until the date of death or the end of follow-up. A univariate analysis of disease-free survival (DFS) was done using the Kaplan–Meier method with a log-rank test, and a multivariate disease survival analysis was carried out under the Cox proportional hazards model. All data were analyzed with JMP for Windows (SAS Institute, Tokyo, Japan).

Results

Relationship between pCR and clinicopathological factors

Thirty-three patients were identified as TNBCs, and the patients' data are shown in Table 1. The age of the patients ranged from 30 to 68 years old (median 50.0) and 21 patients had clinically positive nodes. Clinical response after NAC was rated as clinical complete response for 14 patients (42%), a clinical partial response for 14 patients (42%), a clinical stable disease for 3 patients (9%), and as a clinical progress disease for 2 patients (6%). Also pCR was achieved in only 12 patients (36%).

The correlations between clinicopathological factors such as tumor size, lymph nodal metastasis, age, histological grade, and pCR rate were analyzed (Table 2). However,

Table 1 Patients' characteristics

Variables	No (%)
Total	33
Age: years-old	30–68 (50 ± 11.1)
Histology	
Papillo-tubular	4 (12)
Solid tubular	14 (42)
Schirrous	11 (33)
Special type	4 (13)
T	
1	1 (3)
2	24 (72)
3	6 (18)
4	2 (6)
N	
0	12 (36)
1	17 (52)
2	4 (12)
Histological grade	
1	1 (3)
2	4 (12)
3	27 (81)
Unknown	1 (3)
HER-2	
0	18 (55)
1+	11 (33)
2+	4 (12)
HR (hormone receptor)	
Negative	26 (79)
Weak	7 (21)

T and *N* were defined by the criteria of UICC-breast

HR weak is a tumor with low levels of ER and/or PgR determined by IHC (1–9% weakly positive cells)

Table 2 pCR ratio based on clinicopathologic and immunohistochemistrical factors

Variables	Number (%)	pCR (%)	*P* volume	Odd
Age (years old)				
<50	18 (55)	6 (33)	0.69	
50≤	15 (45)	6 (40)		
Size (cm)				
<5	25 (76)	11 (44)	0.09	5.5
5≤	8 (24)	1 (13)		
N				
Positive	21 (64)	8 (38)	0.78	
Negative	12 (36)	4 (33)		
Histological grade				
1–2	5 (15)	3 (60)	0.26	
3	27 (84)	9 (33)		
HR				
Negative	26 (79)	10 (38)	0.95	
Weak	7 (21)	2 (28)		
HER-2				
0, 1+	29 (88)	9 (31)	0.08	6.67
2+	4 (12)	3 (75)		
p53				
Positive	21 (64)	8 (38)	0.78	
Negative	12 (36)	4 (33)		
Ki-67				
50≤ (high)	20 (61)	10 (50)	*0.04	5.5
<50 (low)	13 (39)	2 (15)		
AR				
Positive	6 (18)	3 (50)	0.45	
Negative	27 (82)	9 (33)		
Basal-like#				
Positive	22 (67)	5 (23)	*0.02	5.9
Negative	11 (33)	7 (64)		
CK5/6				
Positive	14 (42)	2 (14)	*0.02	
Negative	19 (58)	10 (53)		
EGFR				
Positive	18 (55)	4 (22)	0.06	
Negative	15 (45)	8 (53)		

* Statistically significant

\# Basal-like subtype is defined as CK5/4 positive and/or EGFR positive. Thus, CK5/6 was not used for multivariate analysis

these clinicopathological factors did not show any correlation with the pCR rate.

Relationship between pCR, and molecular markers

Next, the correlation between molecular markers and the pCR rate was also analyzed. HER-2 (2+) tended to show a higher pCR rate than HER-2 negative (0 or 1+; 75 and 31%, respectively). In this study, basal markers of CK5/6 and EGFR were evaluated with 22 of 33 patients (67%) diagnosed with basal-like phenotype, and eleven patients (33%) diagnosed with the non-basal-like phenotype. The pCR rate for the basal-like phenotype was significantly lower than in the non-basal-like phenotype (23 and 64%, respectively: $P = 0.02$; Table 2). Ki-67 was also considered as a predictive factor for NAC response, because the pCR rate reaches 50% among high Ki-67 (≥50%) patients, while it was 15% in low Ki-67 patients ($P = 0.04$). The expressions of HR, p53 and AR were not correlated with pCR in this study. Multivariate analysis showed that only high Ki-67 was a significant factor for the prediction of pCR (Table 3). The classification of basal-like or non-basal-like phenotypes was negative for multivariate analysis, probably because high Ki-67 and non-basal-like were strongly correlated with each other; high Ki-67 accounted for 33% in the basal-like and 75% in the non-basal-like phenotype.

Relationship between pCR and disease-free survival

All patients underwent surgical resection after NAC and non-pCR patients were histologically evaluated. The average observation period after surgery was 2 years and eight patients (24%) showed distant metastasis during the observation period. Seven out of 8 patients had been defined as non-pCR and only one patient obtained pCR after NAC. Non-pCR patients showed a worse DFS compared with pCR patients, but it was not statistically significant (Fig. 1a). Basal-like phenotype and other clinicopathological factors such as age, tumor size and lymph nodal involvement failed to show a correlation with DFS (Table 4). Ki-67 before NAC showed a significant correlation with DFS and high Ki-67 patients showed a poor prognosis (Fig. 1b).

Disease-free survival among non-pCR patients

Among non-pCR patients, only 7 patients (29%) showed a recurrence. We analyzed clinicopathological and IHC factors for better prognosis among non-pCR patients. The immunohistological changes of tumors after NAC were

Table 3 Multivariate analysis of pCR and immunopathological factors

Variables	Odds	*P* value
Non-basal-like	3.9	0.13
HER2 (2+)	10.2	0.12
High Ki-67	8.4	0.03*

* Statistically significant

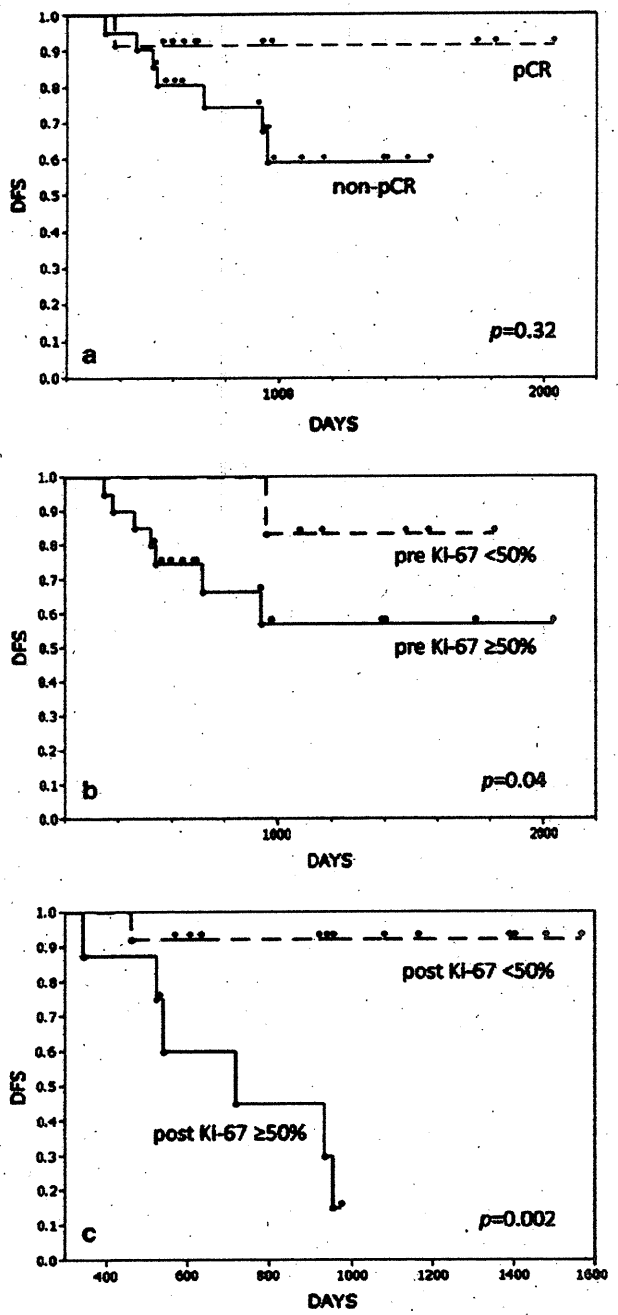

Fig. 1 Disease-free survival (DFS). **a** DFS of pCR and non-pCR patients after NAC. Non-pCR patients showed worse disease-free survival compared with pCR patients, but it was not statistically significant ($P = 0.32$). **b** DFS based on Ki-67 expression of pre-chemotherapy. High Ki-67 (≥50%) patients showed significantly worse disease-free survival than low Ki-67 (<50%) patients ($P = 0.04$). **c** DFS based on Ki-67 expression of post-NAC among non-pCR patients. Non-pCR patients who had high Ki-67 expression after NAC showed a poor prognosis ($P = 0.002$)

evaluated. Among non-pCR patients, 10 patients showed high Ki-67 before chemotherapy and 7 patients still showed high Ki-67 after NAC (Table 5). Among these patients, 6 showed a recurrence and Ki-67 values after NAC were significantly correlated with DFS (Fig. 1c). The expressions of p53 and AR after NAC were not correlated with DFS (data not shown).

Table 4 Multivariate analysis of disease-free survival and patients' characteristics

Variables	Hazard ratio	*P* value
≥50 years-old	0.39	0.2
≥5 cm	2.2	0.3
N positive	4.2	0.11
HR positive	3.2	0.1
HER-2 (2+)	3.2	0.56
Non-basal	1.4	0.6
High Ki-67	5.95	0.04*
p53 positive	0.48	0.3
AR positive	0.000	0.054
Non-pCR	3.7	0.16
High Ki-67 post-NAC#	13.2	0.0029*

Data among non-pCR patients

* Statistically significant

Table 5 The correlation between Ki-67 expression, pCR and the change of Ki-67 expression among non-pCR patients

TNBC ($n = 33$)	Non-pCR		pCR
	Post-NAC Ki-67		
	High	Low	
Pre-NAC Ki-67			
High	7	3	10
Low	1	10	2

Discussion

TNBC is defined by the lack of ER, PgR and HER-2 expression. Because targeted therapies are not useful, chemotherapy is the only systemic treatment option for TNBC [1–5]. Thus, a comprehensive examination of the clinical phenotypes of TNBCs which respond to chemotherapy is important. TNBCs are a heterogeneous group and generally divided into two subtypes; basal-like phenotype and non-basal-like phenotype [6]. The basal-like phenotype is characterized as having a high expression of keratins, laminin, and EGFR.

Many data indicated that the pCR rate is higher in TNBC compared with other phenotypes [10]. A pathological evaluation after NAC is very important because pCR after NAC indicates better survival [8, 9]. Our data showed the pCR rate in TNBCs was 36%, which is consistent with previous